Aging exponents in self-organized criticality

Stefan Boettcher

Center for Theoretical Studies of Physical Systems, Clark Atlanta University, Atlanta, Georgia 30314
and Center for Nonlinear Studies, MS-B258, Los Alamos National Laboratory, Los Alamos, New Mexico 87545

In a recent Letter [Phys. Rev. Lett. **79**, 889 (1997)] we demonstrated that the avalanches in the Bak-Sneppen model display aging behavior similar to glassy systems. Numerical results for temporal correlations show a broad distribution with two distinct regimes separated by a time scale that is related to the age of the avalanche. This dynamical breaking of time-translational invariance results in a previously unrecognized critical exponent r. Here we present results for r from extensive numerical simulations of self-organized critical models in $d = 1$ and 2. We find $r_{d=1} = 0.45 \pm 0.05$ and $r_{d=2} = 0.23 \pm 0.05$ for the Bak-Sneppen model, and our results suggest $r = 1/4$ for the analytically tractable multitrade model in both dimensions. [S1063-651X(97)00812-X]

I. INTRODUCTION

Self-organized criticality (SOC) [1] describes a general property of slowly driven dissipative systems with many degrees of freedom to evolve intermittently in terms of bursts spanning all scales up to the system size. Many natural avalanchelike phenomena have been represented using this concept, including earthquakes [2–4], extinction events in biological evolution [5–7], and landscape formation [8,9]. Recently, SOC has been observed in controlled laboratory experiments on rice piles [10]. Theoretical models of rice piles [11] are related to a variety of different physical systems by universality [12]. One crucial ingredient for a system to exhibit SOC is the existence of thresholds that allow it to record the stress exerted by the driving force over long periods of time. The emergence of long-term memory has been demonstrated analytically [13] for a multitrait evolution model [14], a variant of the Bak-Sneppen model [7].

In a recent Letter [15] we have shown that the self-organized critical state in the Bak-Sneppen model exhibits aging behavior that is reminiscent of glassy systems [16]. Our results indicate that intrinsic two-time autocorrelation functions $P(t_w; t)$, describing the return of activity to a site at time $t_a = t + t_w$ which was active most recently at time $t_a = t_w$ for an avalanche that started at $t_a = 0$, decay as power laws with two distinct regimes according to

$$P(t_w; t) \sim t^{-\tau_{\text{first}}} f\left(\frac{t}{t_w}\right),$$

$$f(x) \sim \begin{cases} \text{const} & (x \ll 1), \\ x^{-r} & (x \gg 1). \end{cases} \tag{1}$$

The early time regime is that of the familiar stationary dynamics. The late time regime has a new critical coefficient r characterizing the nonstationary relaxation behavior of the SOC systems. The "waiting time" t_w separating the early and late time regimes is a measure of the age of the avalanche. We have argued that this aging behavior arises from the hierarchical structure of the avalanches.

Generally, the origin of aging behavior does not have to be profound. For instance, it arises in a simple random walk model near a wall, where a symmetry (translational invariance) is explicitly broken. But while the random walk near a wall and the Bak-Sneppen model (especially its random neighbor variant [17]) are similar in many ways, it appears that those similarities do not explain the observed aging behavior.

In Sec. II, we use the random walk near a wall to illustrate the quantities that will be measured for the SOC models. In Sec. III, we consider the important technical issue of extracting the intrinsic aging behavior for a process that does not conserve its norm (such as a random walk near an absorbing wall or a SOC avalanche, having a finite stopping probability). In Sec. IV, we present detailed numerical results for the aging behavior of SOC models in one and two dimensions. In particular, we have simulated the Bak-Sneppen model and the multitrade model. We have also simulated sandpile models exhibiting SOC that show a quite different behavior and will be discussed elsewhere [18]. Aging in the approach towards or away from the SOC state of sandpile models has also been investigated in Ref. [19]. In Sec. V we discuss our results and show that a simple random walk description is not sufficient to explain the found aging behavior.

II. AGING RANDOM WALKS

In this section we will discuss a random walk model to provide a simple intuitive picture of aging. It shows how the system memorizes the (here, explicit) breaking of a symmetry. Furthermore, the random walk illustrates the meaning of the correlation functions used to describe the aging behavior and serves to discuss some of the technical issues in measuring those functions.

We want to consider a random walker on a $d = 1$ lattice who can jump at most one step on each update either on the infinite lattice or a semi-infinite lattice with an absorbing wall at the origin. A random walk is completely described by its propagator, the conditional probability $G(n, t | n_0, t_0)$ for a walker to reach a site n at time t, given that it was at site n_0 at some previous time $t_0 < t$. To determine its aging behavior we want to compute a simple two-time correlation function (see, e.g., Ref. [20] for a similar definition)

$$P(t_w;t) = \sum_n G(n,t+t_w|n,t_w)G(n,t_w|n_0,0) \qquad (2)$$

for a walker to return to a site at time $t_a = t + t_w$, given that it was at the same site at the "waiting time" t_w after the start of the walk. Thus, to determine the return probability to a site, we take the time t_w from the start of the walk to a previous passage at that site into account. If the two-time correlation function P explicitly depends on t_w, the system is said to "age" because the walk would retain a memory of the time since its inception in form of a return probability that evolves over time.

A. Unconstrained random walks

Clearly, for an unconstrained walk, G is invariant under shifts in space and time, and it is $G(n,t+t_w|n,t_w) = G(0,t|0,0)$. Since the norm of the walk is preserved at all times, $\Sigma_n G(n,t_w|n_0,0) \equiv 1$, Eq. (2) gives $P(t_w;t) \equiv P(t) \equiv G(0,t|0,0)$, independent of t_w. Thus the unconstrained walk has no memory of its past and does not age.

B. Random walks near an absorbing wall

In the presence of an absorbing wall at the origin, spatial invariance is explicitly broken while time invariance for G still holds. Equation (2) merely simplifies to

$$P(t_w;t) = \sum_{n>0} G(n,t|n,0)G(n,t_w|n_0,0), \qquad (3)$$

which remains dependent on t_w. Hence the breaking of spatial invariance in G leads to a breaking of time invariance in P. Such a memory effect arises in the following manner: while in the unconstrained case the mean distance $\langle n \rangle$ of the walker from its origin vanishes, the walker starting near a wall departs from it such that $\langle n \rangle \sim t^{1/2}$, which follows from the propagator given by

$$G(n,t|n_0,0) \approx \frac{1}{\sqrt{\pi t}}[e^{-(n-n_0)^2/4t} - e^{-(n+n_0)^2/4t}] \qquad (4)$$

for sufficiently large t and n. Since the distribution for all walks is sharply peaked near its mean, most walkers occupy sites $n \sim t_w^{1/2}$ away from the wall after the waiting time t_w. *Given* that most walkers occupy such sites n, returns to that site during subsequent times $t \ll t_w$ follow the statistics of an unconstrained walk: t is not yet large enough to return to the wall. Only after times $t \sim t_w$ do a sizable portion of the walkers experience the effect of the distant wall again, which leads to a change in their return statistics for all times $t \gg t_w$. The changeover in its return behavior at later times $t + t_w$ thus provides the walker with a memory of the earlier period from the start up to time t_w when the walk was drifting away from the wall. (Considering the walker as the center of a growing domain and its distance to the wall as a measure of the linear size of that domain relates this random walk model nicely to the domain-growth picture of aging in glasses proposed in Ref. [21].)

For this random walk model the crossover in its return behavior can be easily derived explicitly: inserting the appro-

priate forms of G in Eq. (4) into Eq. (3) and choosing n_0 arbitrarily close to the wall, we obtain asymptotically

$$P(t_w;t) \approx \frac{n_0}{\pi\sqrt{tt_w^3}}\int_0^\infty dn[1-e^{-n^2/t}]ne^{-n^2/4t_w}$$

$$= \frac{n_0}{\sqrt{t_w}}\frac{2}{\pi}t^{-1/2}f\left(\frac{t}{t_w}\right), \quad f(x) = \frac{1}{1+x/4}. \qquad (5)$$

Thus, time-translational invariance is broken and the walk appears to age because P becomes a function of the scaling variable $x = t/t_w$, signaling the predicted crossover in the return behavior that scales linearly with the waiting time t_w. Here the scaling function $f(t/t_w)$ behaves asymptotically as $f(x \ll 1) \sim 1$ and $f(x \gg 1) \sim 4/x$. But to obtain the "intrinsic" aging behavior of this process, we have to consider the effect that the norm is not preserved because at each time step walkers may disappear at the absorbing wall.

III. INTRINSIC VS MEASURED AGING BEHAVIOR

Consider the unconstrained random walk in Sec. II A, but with a finite probability z to disappear at each time step. Then, the propagator G_z of this walk is given by $G_z(n,t|n_0,t_0) = (1-z)^{t-t_0}G(n,t|n_0,t_0)$, where G is the propagator of the norm-preserving walk in Sec. II A. Thus, with $\Sigma_n G(n,t|n_0,t_0) = 1$, we get $\Sigma_n G_z(n,t|n_0,t_0) = (1-z)^{t-t_0}$, i.e., the norm of this process is not preserved. According to our definition of the two-time autocorrelation function P in Eq. (2),

$$P^{\text{meas}}(t_w;t) = \sum_n G_z(n,t+t_w|n,t_w)G_z(n,t_w|n_0,0)$$

$$= G(0,t|0,0)(1-z)^{t+t_w}, \qquad (6)$$

we would have to conclude that this process ages, since P depends on t_w. And, indeed, in a numerical simulation of the process we would measure P^{meas}, because we would average over all processes up to a temporal cutoff t_{co}, including those that disappear at times $t < t_{\text{co}}$.

But, clearly, the "aging" in this simple process is an artifact due to the diminished norm $(1-z)^{t+t_w}$ at time $t + t_w$. Thus, proper normalization is required to extract the "intrinsic" aging behavior (due to the infinite walk) from the "measured" aging behavior [22].

Other processes, such as random walks near an absorbing wall or avalanches in the Bak-Sneppen mechanism below, also may disappear before reaching a cutoff, and we have to consider the effect on the statistics of the measured results. Here, too, one is interested in the intrinsic properties of the surviving process, i.e., those of the infinite random walk or avalanche, while in simulations one usually averages over all runs of a process, whether they survived or not. In many cases, the results for the asymptotic scaling behavior of some intrinsic property are no different from the measured ones because the contribution from dying runs remains insignificant. But for the correlation functions considered in this paper, which depend on two independent time variables, we do

need to consider the effect of the probability $P_t(\theta)$ of a process to disappear at time θ to relate the intrinsic and the measure results.

To obtain the *intrinsic* properties of the infinite process, we have to properly normalize the correlation function. To that end, we consider the two-time correlation function $P(t_w;t|\theta)$ for a run that disappears exactly at time $t_a=\theta$, and its generic relation to the intrinsic two-time correlation function $P^{\text{intr}}(t_w;t)$:

$$P(t_w;t|\theta)=\begin{cases} 0 & (\theta<t_w+t) \\ P^{\text{intr}}(t_w;t) & (\theta\geq t_w+t). \end{cases} \quad (7)$$

These quantities are related to the measured two-time correlation function $P=P^{\text{meas}}$ given in Eq. (5): assuming a power-law probability $P_t(\theta)\sim\theta^{-\tau}$, $\tau>1$, for the run to disappear at time $t_a=\theta$, we have

$$P^{\text{meas}}(t_w;t)=\int_0^{t_{\text{co}}}d\theta\; P(t_w;t|\theta)P_t(\theta)$$

$$\sim P^{\text{intr}}(t_w;t)[(t_w+t)^{1-\tau}-t_{\text{co}}^{1-\tau}]. \quad (8)$$

Assuming that we only consider data sufficiently far from the cutoff, i.e., $(t_w+t)^{1-\tau}\ll t_{\text{co}}^{1-\tau}$, we obtain

$$P^{\text{intr}}(t_w;t)\sim P^{\text{meas}}(t_w;t)(t_w+t)^{\tau-1}. \quad (9)$$

For the particular form of the intrinsic two-time correlation function considered in Eq. (1), the correct scaling function for the aging behavior of the process is given by

$$f^{\text{intr}}(x)\sim f^{\text{meas}}(x)(1+x)^{\tau-1}. \quad (10)$$

Since we are interested in the intrinsic behavior $f^{\text{intr}}(x\gg1)\sim x^{-r}$, we obtain from our numerical data

$$f^{\text{meas}}(x)\sim x^{-(r+\tau-1)}. \quad (11)$$

Of course, for the random walk near the absorbing wall it is $\tau=3/2$ from the familiar first passage time [23]. Thus, even after correcting for the effect of disappearing walkers, the intrinsic process still shows aging behavior: the measurable aging effect derived in Eq. (5), $f(x)=f^{\text{meas}}(x)\sim x^{-1}$, leads to an intrinsic aging behavior of $f^{\text{intr}}(x\gg1)\sim x^{-r}$ with $r=1/2$ according to Eq. (11).

IV. AGING IN SELF-ORGANIZED CRITICAL MODELS

The Bak-Sneppen model [7] has been studied intensely and with great numerical accuracy in recent years. We refer to Ref. [24] for a review of its many features and simply utilize those facts here. The model consists of random numbers λ_i between 0 and 1, each occupying a site i on a d-dimensional lattice. At each update step, the smallest random number $\lambda_{\text{min}}(t)$ is located. That site as well as its $2d$ nearest neighbors each get new random numbers drawn independently from a flat distribution between zero and one. The system evolves to a SOC state where almost all numbers have values above λ_c, with λ_c avalanches formed by the remaining numbers below.

The multitrade model [14,13] is a variant of the Bak-Sneppen model that provides a series of exact results for the spatiotemporal correlations in the avalanche process. In particular, an equation of motion can be derived and solved to obtain a propagator for the spread of avalanche activity, and to obtain a complete set of scaling exponents that verify scaling relations previously proposed for the Bak-Sneppen model. In this model each lattice site is occupied by M independent random numbers. On each update again the smallest number in the whole system is located and updated, and one randomly chosen number (out of M) from each of the neighboring sites is updated as well. While the mechanism proceeds in the same way for all M as for $M=1$ (the Bak-Sneppen model), it can be treated analytically for $M=\infty$.

A quantity similar to the two-time autocorrelation function defined in Eq. (2) can be measured for avalanches in the self-organized critical state of both models. We focus on a simple quantity, $P_{\text{first}}(t)$, measuring the first returns of the activity to a given site. A power law distribution for $P_{\text{first}}(t)$ has been measured numerically for a variety of different SOC models [24] by recording all first returns and its exponent has been derived exactly for the multi-trade model [14]. Here we determine the intrinsic probability $P_{\text{first}}(t_w;t)$ to return after t time steps to a site that was visited most recently at time t_w from the beginning of the avalanche. Thus, to obtain the first-return probability, we take the age of the avalanche, t_w, into account. While in the stationary state of SOC models the first return distribution is generally $P_{\text{first}}(t)\sim t^{-\tau_{\text{first}}}$ $(t\to\infty)$, we find that $P_{\text{first}}(t_w;t)$ for both models considered here scales according to Eq. (1) where the exponent τ_{first} can be related to other critical exponents via scaling relations for SOC [24]. The origin of the intrinsic aging exponent r appears to us to be nontrivial, signaling the breaking of time-translational invariance in the avalanche dynamics. Unlike in the random walk near a wall, no symmetry is explicitly broken. The Bak-Sneppen mechanism in both models evolves on an isotropic lattice with update rules that do not change with time. The question then arises whether the exponent r in Eq. (1) can be related to the known universal coefficients of the stationary SOC process, or whether it describes new physics in avalanche dynamics of the Bak-Sneppen model.

A. Numerical procedure

In our simulations for both models we have used the equivalent branching process [25] to eliminate any finite-size effects. Initially, at time $t_a=0$, the smallest threshold value is set equal to λ_c to start a λ_c avalanche. In every update $t_a\to t_a+1$, only the signal $\lambda_{\text{min}}(t_a)$ and its $2d$ nearest-neighbor sites receive new threshold values. At any time, we store only those threshold values $\lambda_i<\lambda_c$ that are part of the avalanche because only those numbers can contribute to the signal, i.e., can ever become the smallest number. In addition, we keep a dynamic list of every site that has ever held the signal at some time to determine the first-return probabilities. (Since the Bak-Sneppen mechanism for $d<4$ is a fractal renewal process, activity always returns to a site unless the avalanche dies.) Avalanches die when there are no $\lambda_i<\lambda_c$ or are stopped at a cutoff $t_a=t_{\text{co}}$, and a new (independent) avalanche is initiated with $t_a=0$.
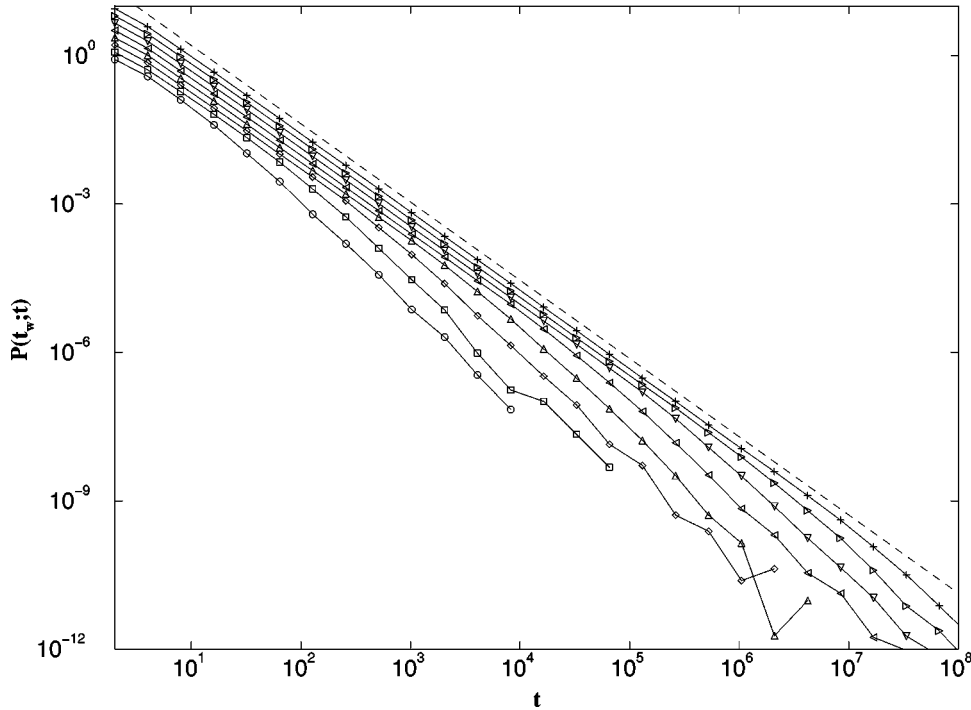
FIG. 1. Plot of $P_{\text{first}}^{\text{meas}}(t_w;t)$ as a function of t for the Bak-Sneppen model in $d=1$. Each graph is offset by a factor to avoid overlaps.

At each update t_a we determine the previous time t_w when the signal was on the same site most recently (if ever). Then its first-return time is given by $t=t_a-t_w$, and we bin histograms labeled by $i=\lceil\frac{1}{3}\log_2 t_w\rceil$ and $j=\lceil\log_2 t\rceil$. The data are binned logarithmically so that in each bin a comparable number of events is averaged over: for each increment of j, the width of the bins for t increases by a factor of 2, while for each increment of i the t_w bins increase by a factor of 8. We then normalize for each value of i separately to obtain the measured first-return probabilities $P_{\text{first}}^{\text{meas}}(t_w;t)$. These

data are plotted in Figs. 1, 3, 5, and 7.

In each figure, each graph refers to a different value of i, increasing by a factor of 8 each time from left to right. Each graph possesses two distinct power law regimes, separated by a crossover. To determine the form of the scaling function $f(x)$ for these graphs according to Eqs. (1), we note that the crossover appears to scale linearly with t_w in all cases. Thus, we plot

$$f^{\text{meas}}(x)\sim t^{\tau_{\text{first}}}P_{\text{first}}^{\text{meas}}(t_w;t), \quad x=\frac{t}{t_w}, \tag{12}$$
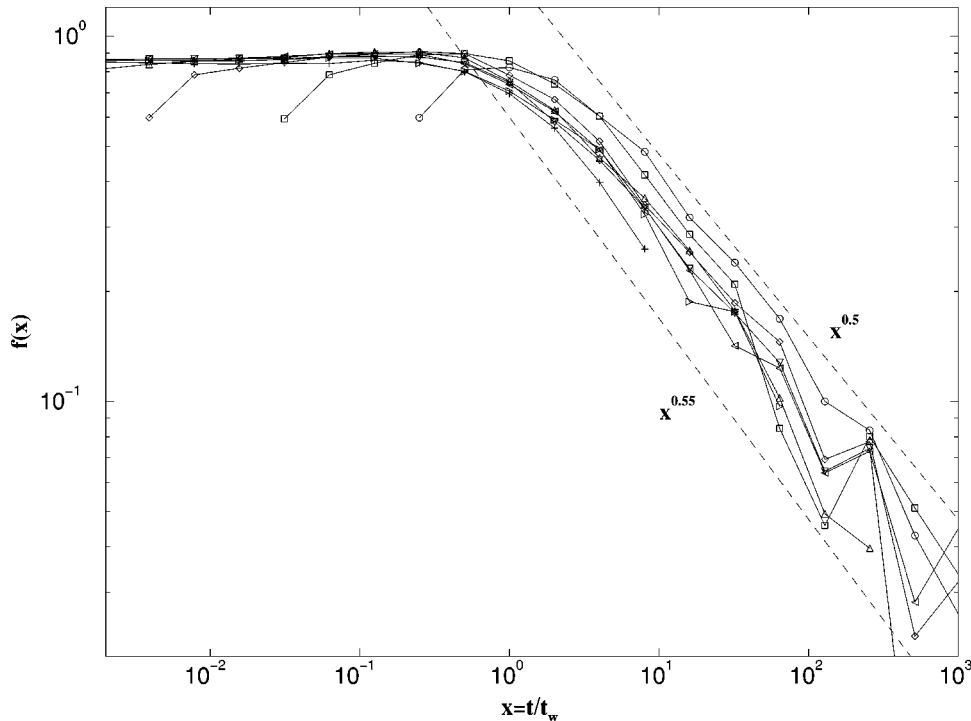

FIG. 2. Scaling plot for $f^{\text{meas}}(x)$ as a function of $x=t/t_w$ according to Eq. (12) for the normalized distribution of the $1d$ Bak-Sneppen model in Fig. 1.
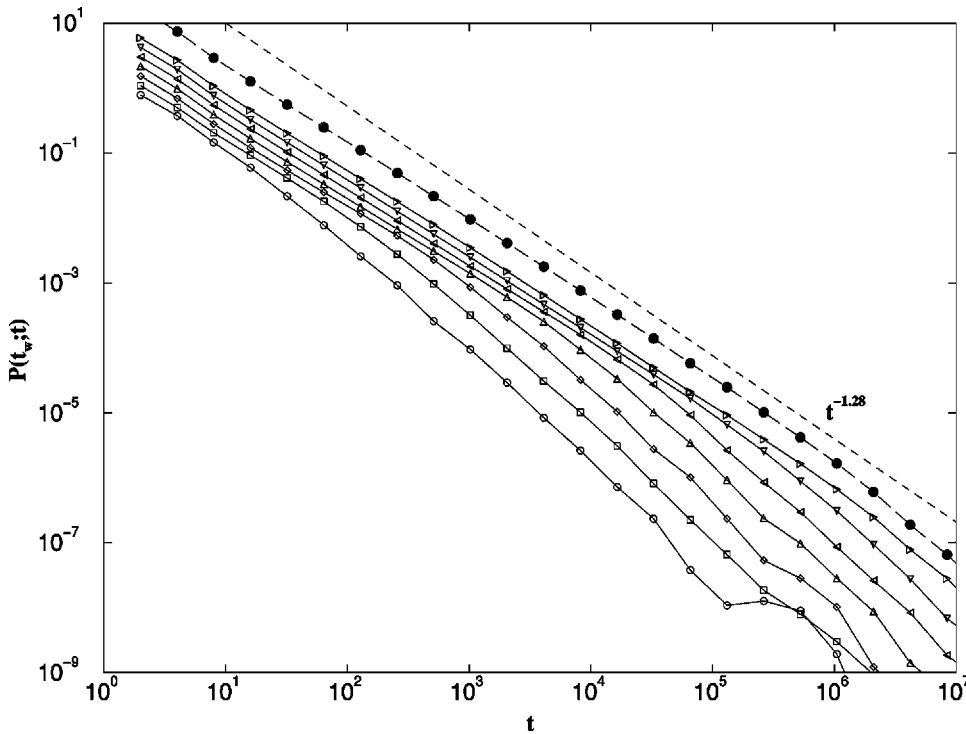
FIG. 3. Plot of $P_{\text{first}}^{\text{meas}}(t_w;t)$ as a function of t for the Bak-Sneppen model in $d=2$. Each graph is offset by a factor to avoid overlaps.

using the appropriate values of τ_{first}. In each case, the data collapse reasonably well onto a single curve, $f(x)$, which is constant for small argument, and appears to fall like a power law, see Figs. 2, 4, 6, and 8. The exponent of the power law is given by $r+\tau-1$ according to the relation between measured and intrinsic data discussed in Sec. III [see Eq. (11)]. The values of τ are given in Ref. [24] for the Bak-Sneppen model in $d=1$ and 2, and $\tau=3/2$ in any dimension for the multitrade model.

We have simulated the Bak-Sneppen branching process in $d=1$ with $\lambda_c=0.66702$, summing over a sequence of all avalanches up to a cut-off at $t_{\text{co}}=2^{27}$. That data consist of a total of about 10^{11} updates. (The results reported here are consistent with but substantially better than those reported previously in Ref. [15] where data from avalanches that did not reach the cutoff were discarded to avoid confusion about the relation between measured and intrinsic properties discussed in Sec. III.)

The distributions for $P_{\text{first}}^{\text{meas}}(t_w;t)$ as a function of t, normalized for each value of i, $8^{i-1}\leq t_w<8^i$, are plotted in Fig. 1 for $i=1,\ldots,8$. Each graph shows two scaling regimes separated by a crossover that appears to scale linearly with
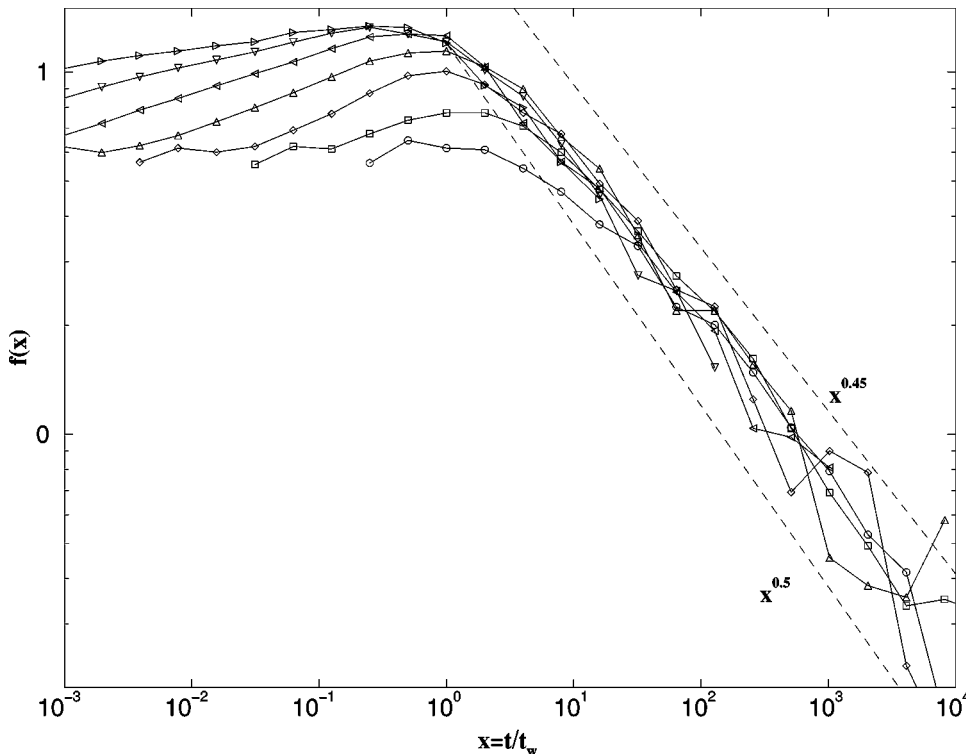

FIG. 4. Scaling plot for $f^{\text{meas}}(x)$ as a function of $x=t/t_w$ according to Eq. (12) for the normalized distribution of the $2d$ Bak-Sneppen model in Fig. 3.
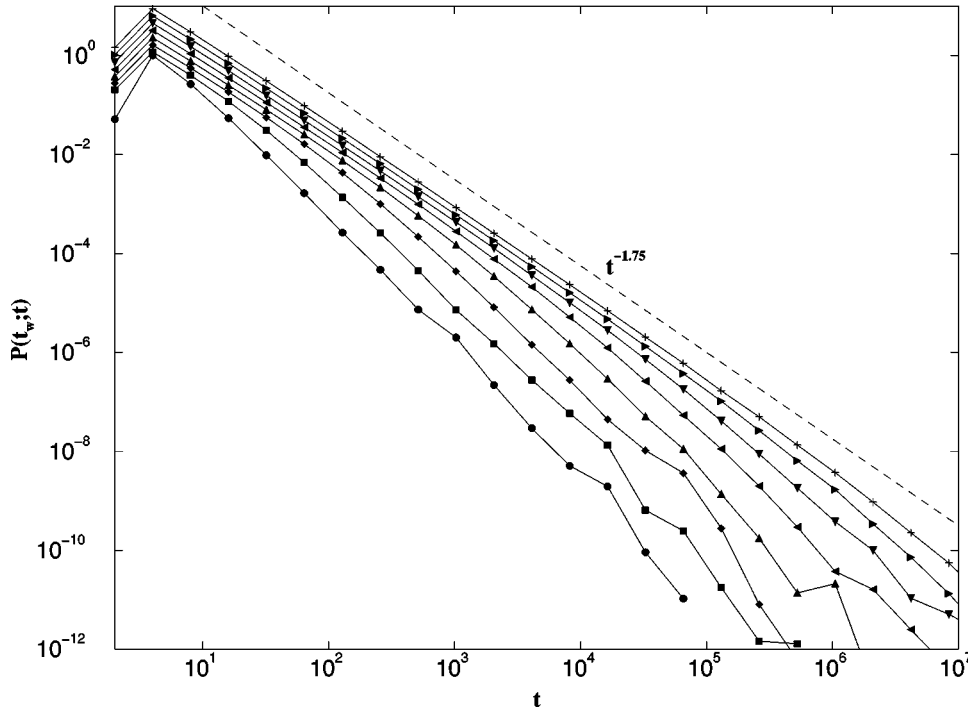
FIG. 5. Plot of $P_{\text{first}}^{\text{meas}}(t_w;t)$ as a function of t for the multitrade model in $d=1$. Each graph is offset by a factor to avoid overlaps.

the associated value of t_w. The initial regime scales with the familiar exponent $\tau_{\text{first}}=1.58$ [24] (as indicated by the dashed line to the right). Cutoff effects become apparent at about $t\approx 10^7=10\% \, t_{\text{co}}$.

In Fig. 2 we have combined the data into a scaling plot for $f^{\text{meas}}(x)$ according to Eq. (12) as a function of the scaling variable $x=t/t_w$. For $x<1$ that data indeed collapse onto a constant, while we observe a collapse onto a power law over three orders of magnitude for $x>1$. Deviations from this behavior are generally due to short-time, transient behavior for $x<1$, and due to statistical noise deep in the tail of the distribution for $x>1$. We have bracketed the power law tail

by two dashed lines $\sim x^{-0.55}$ and $\sim x^{-0.5}$. Thus, we estimate that the exponent of the tail is given by $r+\tau-1=0.52 \pm 0.04$. With $\tau=1.07\pm 0.01$ [24], we finally get $r=0.45 \pm 0.05$.

B. Results for the Bak-Sneppen model in $d=2$

In this case we have simulated the branching process with $\lambda_c=0.328\,855$ [24], summing over a sequence of all avalanches up to a cutoff at $t_{\text{co}}=2^{25}$ (longer avalanches are less common here than in the $d=1$ case). We have run about 3×10^{10} updates for this model.
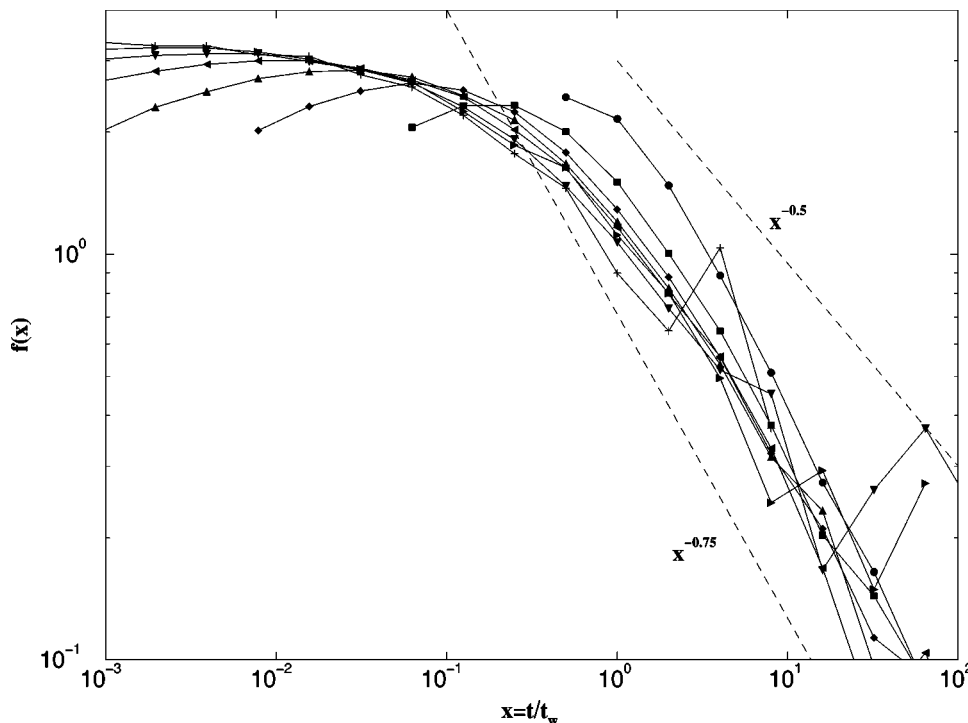

FIG. 6. Scaling plot for $f^{\text{meas}}(x)$ as a function of $x=t/t_w$ according to Eq. (12) for the normalized distribution of the $1d$ multitrade model in Fig. 5.
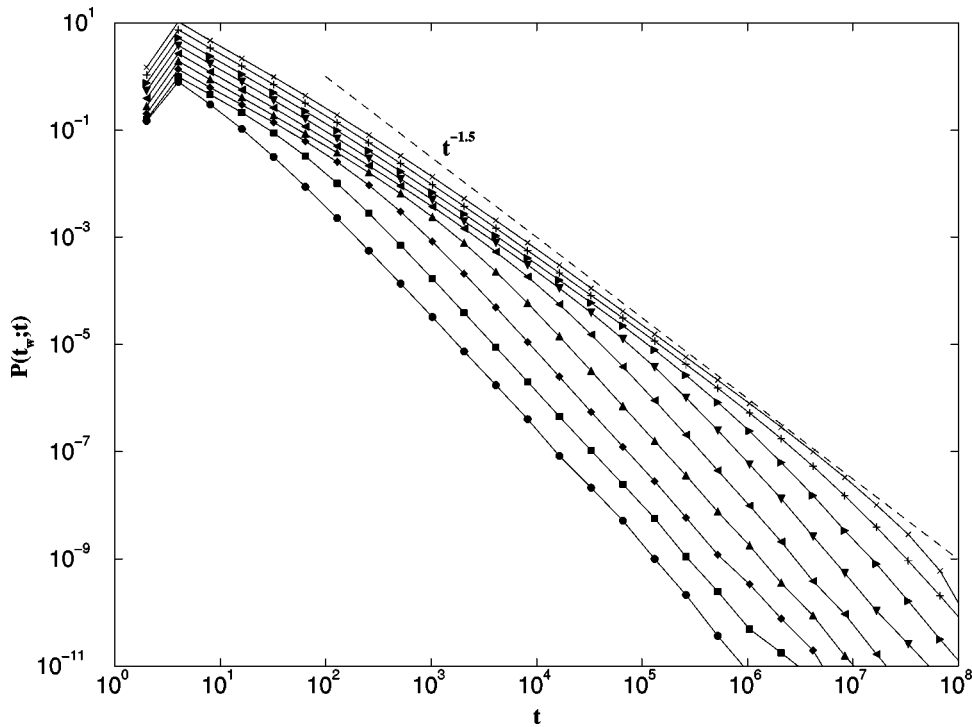
FIG. 7. Plot of $P_{\text{first}}^{\text{meas}}(t_w;t)$ as a function of t for the multitrade model in $d=2$. Each graph is offset by a factor to avoid overlaps.

The distributions for $P_{\text{first}}^{\text{meas}}(t_w;t)$ as a function of t, again normalized for each value of i, $8^{i-1} \leq t_w < 8^i$, are plotted in Fig. 3 for $i=1,\ldots,7$. As in the $d=1$ case, each graph shows two scaling regimes separated by a crossover that appears to scale linearly with the associated value of t_w. The initial regime supposed to scale with the exponent $\tau_{\text{first}}=1.28$ determined from a more extensive simulation in Ref. [24]. That behavior is given by the dashed line to the right. But each graph approaches that asymptotic behavior in its initial scaling regime only very slowly, indicating strong corrections to scaling in this case. Even the combined data (the dashed line

with circular marks), not unlike the corresponding plot in Ref. [24], approach the asymptotic behavior only very slowly. Furthermore, cutoff effects become apparent at about $t \approx 10^6 = 10\% \, t_{\text{co}}$.

In Fig. 4 we have combined the data into a scaling plot for $f^{\text{meas}}(x)$ according to Eq. (12) as a function of the scaling variable $x=t/t_w$. The collapse onto a constant for the data at $x<1$ only proceeds slowly due to the aforementioned corrections to scaling in the first return probability. On the other hand, we observe a collapse onto a power law over more than three orders of magnitude for $x>1$ in this case: since
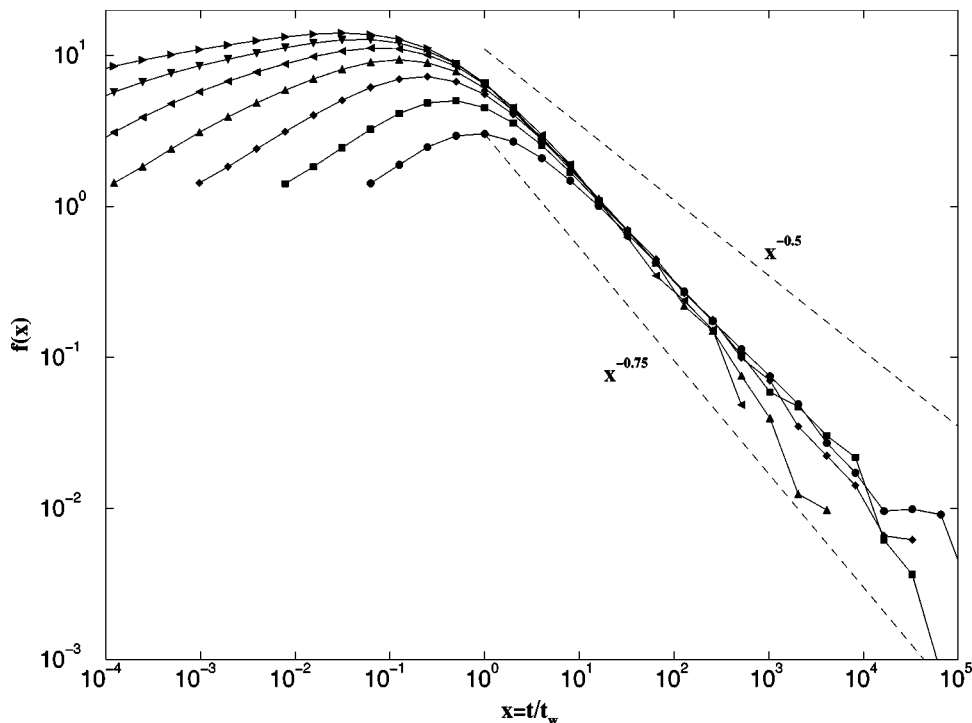

FIG. 8. Scaling plot for $f^{\text{meas}}(x)$ as a function of $x=t/t_w$ according to Eq. (12) for the normalized distribution of the $2d$ multitrade model in Fig. 7.

$\tau_{\text{first}} = 1.28$ is smaller than in the case $d = 1$, many more events occur in the tail of the distribution. We have bracketed the power law tail by two dashed lines $\sim x^{-0.5}$ and $\sim x^{-0.45}$. Thus, we estimate that the exponent of the tail is given by $r + \tau - 1 = 0.47 \pm 0.04$. With $\tau = 1.245 \pm 0.010$ [23], we finally get about $r = 0.23 \pm 0.05$.

C. Results for the multitrade model in $d = 1$

A number of important properties, such as the distributions of the width and duration of an avalanche and the exponent for the avalanche dimension ($D = 4$), can be derived exactly for the multitrade model [14,13]. But many other properties are as of yet elusive or can only be inferred from scaling relations; for instance,

$$\tau_{\text{first}} = 2 - \frac{d}{4}. \qquad (13)$$

In particular, no expression for $P_{\text{first}}(t_w; t)$ has been obtained so far to study the aging behavior in this model more explicitly. Thus, as a first step to obtain an explicit expression, we have simulated this model also in $d = 1$ and 2. The results suggest that $r = 1/4$ in both cases, independent of dimension.

We have simulated the branching process with $\lambda_c = 1/2$ since we chose to update only one number on each neighbor and always replace the minimum itself with 1 [14]. Summing over a sequence of all avalanches up to a cutoff at $t_{\text{co}} = 2^{27}$, we have run about 10^{12} updates for this model.

The distributions for $P_{\text{first}}^{\text{meas}}(t_w; t)$ as a function of t, again normalized for each value of i, $8^{i-1} \leqslant t_w < 8^i$, are plotted in Fig. 5 for $i = 1, \ldots, 8$. Each graph shows two scaling regimes separated by a crossover that appears to scale linearly with the associated value of t_w. According to Eq. (13), the initial regime is known to scale asymptotically with the exponent $\tau_{\text{first}} = 7/4$. That behavior is given by the dashed line to the right. But as in the case of the $2d$ Bak-Sneppen model we observe strong corrections to scaling. Even worse, cutoff effects already become apparent at about $t \approx 10^6 = 1\% \, t_{\text{co}}$. Generally, despite spending much more time on the simulation, the data have the poorest quality in this case also because the large value of τ_{first} suppresses the occurrence of events in the long-time tail.

Nontheless, in Fig. 6, we have combined the data into a scaling plot for $f^{\text{meas}}(x)$ according to Eq. (12) as a function of the scaling variable $x = t/t_w$. As expected, the corrections to scaling prevent a satisfactory collapse onto a constant for the data at $x \ll 1$. Apparently, even the crossover regime is beset by transient behavior, which makes it difficult to localize the transition to the power-law regime. At best, we can discern scaling over two orders of magnitude in the tail before the data get too noisy. On the other hand, it is fair to assume from the analytical results that any exponent in this model should be a multiple of 1/4. Considering that the tail clearly scales very close to the dashed line with $x^{-0.75}$ below and definitely not like the dashed line with $x^{-0.5}$ above, we believe that $r + \tau - 1 = 3/4$. Thus, with $\tau = 3/2$ [14], we conjecture $r = 1/4$.

D. Results for the multitrade model in $d = 2$

We have simulated the branching process with $\lambda_c = 1/4$ since we chose to update only one number on each neighbor

and always replace the minimum itself with 1. Summing over a sequence of all avalanches up to a cutoff at $t_{\text{co}} = 2^{27}$, we have run about 10^{11} updates for this model.

The distributions for $P_{\text{first}}^{\text{meas}}(t_w; t)$ as a function of t, again normalized for each value of i, $8^{i-1} \leqslant t_w < 8^i$, are plotted in Fig. 7 for $i = 1, \ldots, 9$. Each graph shows two scaling regimes separated by a crossover that appears to scale linearly with the associated value of t_w. According to Eq. (13), the initial regime is assumed to scale with the exponent $\tau_{\text{first}} = 3/2$. That behavior is given by the dashed line to the right. We observe again strong corrections to scaling and cutoff effects already at about $t \approx 10^6 = 1\% \, t_{\text{co}}$.

Combining the data into a scaling plot again (see Fig. 8), the corrections to scaling again prevent a satisfactory collapse onto a constant for the data at $x \ll 1$. But we observe an excellent collapse of the data in the tail over roughly three to four orders of magnitude, clearly closer to the dashed line with $x^{-0.75}$ below than the dashed line with $x^{-0.5}$ above. Thus we have $r + \tau - 1 = 3/4$ and $\tau = 3/2$ as well in this case, leading us once more to conjecture $r = 1/4$.

V. CONCLUSIONS

In conclusion, our numerical simulations affirm the existence of a new and as-of-yet unexplained power law regime in the late time behavior of the Bak-Sneppen model that was discovered in Ref. [15]. The results underscore the prevalence of memory effects in the SOC state of this model [13,26] and possibly other SOC models [18].

We have been able to rule out a simple relation of the exponent r to the known exponents by considering some of the more obvious scaling arguments (which may not exist at all) [15]. For instance, we can consider an avalanche as a random walk near a wall in an abstract random number space [17]. The addition or elimination of a random number below the threshold λ_c corresponds to taking a step away or towards an absorbing wall in a random walk. The avalanche ends when no random numbers are left below λ_c, i.e., the walker has been absorbed at the wall. The growth of random numbers below λ_c scales like $\langle n \rangle \sim t^{d_s}$ for the (intrinsic) infinite avalanche, with $d_s = 0.11$ and 0.25 for the $1d$ and $2d$ Bak-Sneppen model [24] and $d_s = 1/2$ for the multitrade model in any dimension. If the aging behavior in these models were due to the same effect as in our simple random walk model in Sec. II, we would expect that $r = d_s$, which is inconsistent with the numerical results. It appears that the origin of the aging behavior is due to more subtle features of the process and that time-translational invariance might be broken dynamically, as we have argued in Ref. [15]. The fact that the analytically tractable multitrade model also shows nontrivial aging behavior gives us hope that we will be able eventually to understand its origin.

[1] P. Bak, C. Tang, and K. Wiesenfeld, Phys. Rev. Lett. **59**, 381 (1987); Phys. Rev. A **38**, 364 (1988).

[2] B. Gutenberg and C. F. Richter, Ann. Geofis. **9**, 1 (1956).

[3] P. Bak and C. Tang, J. Geophys. Res. B **94**, 15 635 (1989); Z. Olami, H. J. S. Feder, and K. Christensen, Phys. Rev. Lett. **68**, 1244 (1992); K. Christensen and Z. Olami, Phys. Rev. A **46**, 1829 (1992); J. Carlson and J. Langer, Phys. Rev. Lett. **62**, 2632 (1989).

[4] K. Ito, Phys. Rev. E **52**, 3232 (1995).

[5] D. M. Raup, Science **231**, 1528 (1986); J. J. Sepkoski, Paleobiology **19**, 43 (1993).

[6] S. J. Gould and N. Eldredge, Paleobiology **3**, 114 (1977); Nature (London) **366**, 223 (1993).

[7] P. Bak and K. Sneppen, Phys. Rev. Lett. **71**, 4083 (1993).

[8] E. Somfai, A. Czirok, and T. Vicsek, J. Phys. A **27**, L757 (1994).

[9] For a review see P. Bak, *How Nature Works: The Science of Self-Organized Criticality* (Copernicus, New York, 1996).

[10] V. Frette, K. Christensen, A. Malthe-Sørenssen, J. Feder, T. Jøssang, and P. Meakin, Nature (London) **379**, 49 (1996).

[11] K. Christensen, A. Corral, V. Frette, J. Feder, and T. Jøssang, Phys. Rev. Lett. **77**, 107 (1996).

[12] M. Paczuski and S. Boettcher, Phys. Rev. Lett. **77**, 111 (1996).

[13] S. Boettcher and M. Paczuski, Phys. Rev. E **54**, 1082 (1996).

[14] S. Boettcher and M. Paczuski, Phys. Rev. Lett. **76**, 348 (1996).

[15] S. Boettcher and M. Paczuski, Phys. Rev. Lett. **79**, 889 (1997).

[16] H. Rieger, J. Phys. A **26**, L615 (1993); Physica A **224**, 267 (1996); for a recent review of aging in glasses, see E. Vincent, J. Hammann, M. Ocio, J.-P. Bouchaud, and L. F. Cugliandolo, in *Proceedings of the Sitges Conference on Glassy Systems*, edited by E. Ruby (Springer, Berlin, 1996); e-print cond-mat/9607224.

[17] J. de Boer, B. Derrida, H. Flyvbjerg, A. D. Jackson, and T. Wettig, Phys. Rev. Lett. **73**, 906 (1994).

[18] S. Boettcher and M. Paczuski (unpublished).

[19] A. Vazquez, O. Sotolougo-Costa, and F. Brouers, e-print cond-mat/9710067.

[20] P. Sibani and K. H. Hoffmann, Phys. Rev. Lett. **63**, 2853 (1989); K. H. Hoffmann and P. Sibani, Phys. Rev. A **38**, 4261 (1988).

[21] G. J. M. Koper and H. J. Hilhorst, J. Phys. (Paris) **49**, 429 (1988); D. S. Fisher and D. Huse, Phys. Rev. B **38**, 373 (1988); see also K. H. Fisher and J. A. Hertz, *Spin Glasses* (Cambridge University Press, Cambridge, 1991).

[22] We believe that it is incorrect to interpret the loss of norm as an aging phenomenon as attempted in D. A. Stariolo, Phys. Rev. E **55**, 4806 (1997).

[23] B. D. Hughes, *Random Walks and Random Environments* (Clarendon, Oxford, 1995).

[24] M. Paczuski, S. Maslov, and P. Bak, Phys. Rev. E **53**, 414 (1996).

[25] M. Paczuski, S. Maslov, and P. Bak, Europhys. Lett. **27**, 97 (1994).

[26] M. Marsili, G. Caldarelli, and M. Vendruscolo, Phys. Rev. E **53**, R13 (1996).